

Development and Validation of High Precision Thermal, Mechanical, and Optical Models for the Space Interferometry Mission

Chris A. Lindensmith, H. Clark Briggs, Yuri Beregovski, V. Alfonso Feria, Renaud Goullioud,
Yekta Gursel, Inseob Hahn, Gary Kinsella, Matthew Orzewalla, Charles Phillips
California Institute of Technology, Jet Propulsion Laboratory
4800 Oak Grove Dr
Pasadena, CA 91109
818-354-6697
lindensm@mail.jpl.nasa.gov

Abstract—SIM Planetquest (SIM) is a large optical interferometer for making microarcsecond measurements of the positions of stars, and to detect Earth-sized planets around nearby stars. To achieve this precision, SIM requires stability of optical components to tens of picometers per hour.

The combination of SIM's large size (9 meter baseline) and the high stability requirement makes it difficult and costly to measure all aspects of system performance on the ground. To reduce risks, costs and to allow for a design with fewer intermediate testing stages, the SIM project is developing an integrated thermal, mechanical and optical modeling process that will allow predictions of the system performance to be made at the required high precision. This modeling process uses commercial, off-the-shelf tools and has been validated against experimental results at the precision of the SIM performance requirements.

This paper¹² presents the description of the model development, some of the models, and their validation in the Thermo-Opto-Mechanical (TOM3) testbed which includes full scale brassboard optical components and the metrology to test them at the SIM performance requirement levels.

This research was carried out at the Jet Propulsion Laboratory, California Institute of Technology, under a contract with the National Aeronautics and Space Administration.

Reference herein to any specific commercial product, process, or service by trade name, trademark, manufacturer, or otherwise, does not constitute or imply its endorsement by the United States Government or the Jet Propulsion Laboratory, California Institute of Technology.

TABLE OF CONTENTS

1. INTRODUCTION	1
2. THERMO OPTO MECHANICAL TESTBED.....	2
3. MODELING ISSUES FOR HIGH PRECISION	3

¹ 0-7803-8870-4/05/\$20.00© 2005 IEEE

² IEEEAC paper #1484, Version 1.0, Updated 19 October, 2005 11:00

4. DEVELOPMENT OF THE SIM MODELS.....	4
5. COMPRESSOR MODEL AND VALIDATION.....	5
6. SIDEROSTAT MODELING AND VALIDATION.....	9
7. CONCLUSIONS	12
REFERENCES.....	13
BIOGRAPHY.....	13

1. INTRODUCTION

SIM [1, 2] is an interferometry mission that is a key element of NASA's search for earth-like planets and life. The SIM instrument is an optical interferometer system with a baseline of 9 m, and includes two "guide" interferometers for spacecraft pointing reference and a "science" interferometer to perform astrometric measurements on target stars.

All three interferometers are similar; the science interferometer consists of two collector telescopes, each of which is composed of a 35 cm diameter flat siderostat (SID) that pivots to change target stars, and a compressor telescope (CMP) that accepts the 35 cm beam from the SID and reduces it to 5 cm, sending a collimated beam to the combiner via a steering mirror and relay optics. In the center of the SID is a double cube-corner (DCC) that serves as a fiducial for the metrology system that determines the pathlength differences in the interferometer.

The DCC is aligned very precisely so that its vertex is within a few micrometers of the front surface plane of the SID flat, and centered on the diameter of the mirror. The pathlength changes of the siderostats in each interferometer must be known to tens or hundreds of picometers, depending on the type of observation. This precision requirement means that the position of the DCC relative to the SID flat must be very stable, because once SIM is on-orbit and operating, the DCC provides the reference point for the position of each of the siderostats and there is no independent way to verify the position of the DCC relative to the flat surface of the SID.

The TOM3 testbed was developed as part of a series of testbeds to both show that this level of stability is achievable and that its performance can be accurately modeled. The modeling aspect is particularly important

because of the physical size and required precision of SIM: full scale tests of such a system will be very expensive, and accurate models can reduce the number or size of tests while maintaining high reliability and acceptable risk.

2.THERMO OPTO MECHANICAL TESTBED

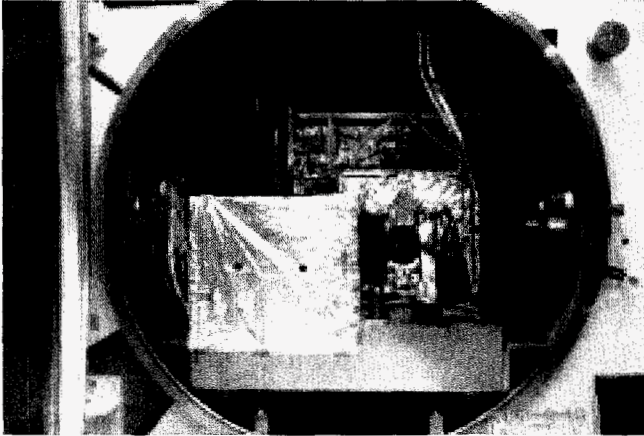


Figure 1 – TOM3 Testbed in Test Chamber.

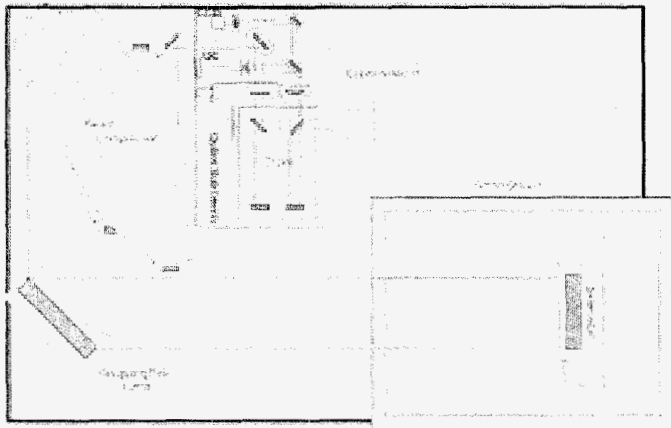


Figure 2 – TOM3 Testbed Layout. The chopping/fold mirror can be used as shown to measure the Beam Compressor and Siderostat simultaneously or rotated counterclockwise into retro mode to measure the Beam Compressor only.

The TOM3 tested (Figure 1) was developed to demonstrate that the required performance could be achieved using brassboard hardware in a flight-like thermal environment and to show that the performance could be predicted accurately enough with integrated modeling tools to enable greater use of integrated models in the flight system development [3]. The performance demonstration was part of a technology milestone for SIM, referred to as Milestone 8, and is discussed elsewhere in these proceedings [4].

The testbed consists of the two brassboard test articles (SID and CMP), a metrology system (COPHI), a chopping/fold mirror (CM), and a thermal shroud for

controlling the environment around the SID. The optical components are mounted rigidly to a 3.3x2.1 m optical bench located inside a large vacuum chamber. The layout is shown in Figure 2. The optical bench is supported within the chamber by four air isolation legs that are outside the chamber. Soft bellows feedthroughs in the chamber allow the air isolators to remain outside the chamber without sacrificing isolation. The thermal shroud is mounted to the chamber wall and does not come in contact with the optical table or any optical components. Cutouts in the lower panel of the shroud allow the bipods supporting the SID to pass through without contacting the shroud.

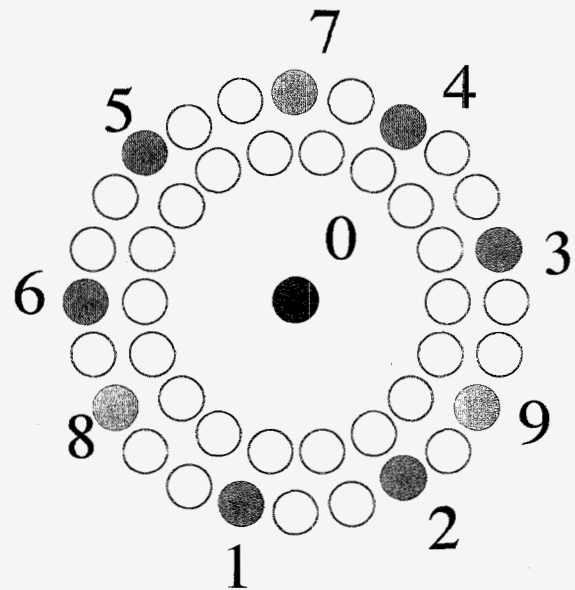


Figure 3 – COPHI Detector Map. Detectors 1-6 are the set of detectors for a single multiplexer (MUX) setting. The different MUX settings are similarly arranged to make distributed measurements of the target. Detectors 7-9 are read continuously and are also included in the multiplexer readout.

The thermal shroud consists of an outer aluminum shell with tubing brazed onto it for liquid or gaseous nitrogen to be used in controlling the shroud temperature, and 12 inner panels painted black to provide a predictable emissivity and fitted with film heaters over their areas to provide stable, uniform temperature control. The inner panels are fitted so that gaps between them are minimized so that the SID has very little view to the outer shroud; the SID environment is determined by the temperature of the inner panels. The shroud panels on the CM side have a hole just large enough to allow the measurement beam from COPHI to pass through. The inner panel on that end of the shroud is normally operated near 80 K to simulate the view to cold space. The length of the shroud is designed to provide view factors to the shroud and the CM that are close to those that the SID will see in the flight system.

The metrology system is a common-path heterodyne interferometer (COPHI) [5,6] that is capable of measuring changes in the optical path difference (OPD) of points in its beam to the precision required for SIM. When data are processed according to SIM narrow angle requirements, COPHI has a noise floor of about 3 pm, and when processed according to SIM wide angle requirements COPHI has a noise floor of about 34 pm. During much of the data acquisition for these tests the effective noise floor was 1.5-3x higher due to an apparent cyclic error source that is believed to be related to thermal variations in the optical fibers feeding the COPHI laser beams into the chamber.

In the TOM3 system COPHI is fitted with 43 detectors: 1 central detector that maps onto the DCC and 42 arranged in two concentric rings (Figure 3) that map onto the SID face. The electronics system is set up to measure OPD changes between the central detector and each of the peripheral detectors. The peripheral detectors are connected such that three detectors 120 degrees apart are read out constantly to use for pointing error measurements, while the remaining detectors are grouped in seven sets of six that can be selected with a multiplexer. The three constant-read detectors are also included in the multi-plexed groups for convenience in data storage and analysis.

3. MODELING ISSUES FOR HIGH PRECISION

Though the stability requirements for SIM appear daunting, the thermo/opto/mechanical modeling for the TOM3 testbed was done with commercial, off-the-shelf tools that were integrated via a "bucket brigade" process. In the bucket brigade each of the discipline analysis was applied sequentially, with the output of one modeling tool used to supply the input to the next tool. This is shown in Figure 4.

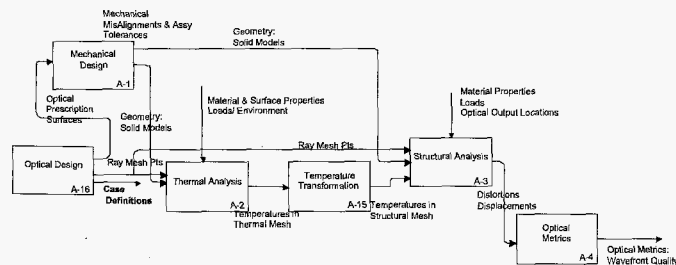


Figure 4 – Integrated Modeling Flow.

Although the ultimate precision of the OPD changes that must be modeled is very high, the physical and temporal scales of the system make it amenable to the application of conventional methods. The picometer precision is measured on large, massive systems (relative to pm) over long times (30 s to 1 h) so that the atomic-level fluctuations that are sometimes brought up as a concern are averaged out and can be ignored. Additionally, the

data optical data are post-processed to remove some types of common mode or systematic errors.

Because classical physics can be used, the physical phenomena involved are well understood: the thermal transport is largely radiation with some contribution from conduction, the structural deformations are caused by temperature-induced strains and are well within the small deformation range of continuum mechanics, the optical effects are well described by geometric optics for computation of the OPD.

The resulting equations are solved by standard methods implemented by the COTS tools and no special selections or set up were required. The thermal equations solution process was watched carefully for signs of numerical instability caused by the potential lack of significant digits in the double precision implementation but none were observed. The solutions were reasonable and well behaved. The solver logs did not indicate any difficulty with solution convergence and run times were not unreasonable.

Mechanical design was done in I-deas [7]. Temperature predictions were made using TMG [8] and transferred directly into an Ideas structural deformations model in order to calculate the resulting mirror wave-front error or OPD. This OPD prediction was then transferred over to an Optics model in CODE-V [9] to predict optical performance. For the most critical temperatures, the SID mirror, DCC, and DCC post, the same finite element mesh was used in both the structural and thermal models so that there would be no interpolation error. A specialized MATLAB script was developed on the structures side to read in raw TMG output files to ensure that the results were read back into the structures model in double precision (the Ideas post processing environment reduces the number of significant digits used in the TMG solver).

The extremely high precision required accurate geometry modeling. This involved aspects of using the correct design models, capturing all significant components, and enveloping the component volumes in elements with significant completeness. This is a very manual process for the most part, although the TC Eng PDM system simplified gaining access to the correct design model. The analysts used manual version control of the abstracted geometry models, the numerical models and the results sets since practices for managing these datasets in TC Eng were not established. In addition to capturing the component volumes, the thermal analyst needed to capture the radiation view factors to better than 99% and this was monitored with reports in the solution logs.

Accounting for the multitude of interfaces was manual and tedious, but the model assembly process provides several checks. Many of the thermal conductances and all the radiation view factors are non-geometric elements manually generated, as are the inter-component conductances. Similarly for the structural models, the

enforcement of compatibility between components is a manual meshing step, but omissions show up prominently.

Material Properties

Material properties were among the largest sources of uncertainty in the TOM3 modeling process. Common materials, such as aluminum and steel are fairly well understood but were not suitable for the SIM optical systems. Primary material properties of interest for the TOM3 modeling are coefficient of thermal expansion (CTE), Young's modulus (E) and Poisson's ratio. Temperatures create strain via CTE. All three properties appear linearly in structural equations. Young's Modulus E varies +/- 5% across lots, although values are not tabulated in Mil-HDBK-5.

Athermal materials such as ULE, Zerodur, invar, which were used in the SIM hardware, are often "tuned" for particular characteristics at in a specified environment. For example, the coefficient of thermal expansion for ULE glass may be 0+-20 ppb at a specified temperature, but there can also be significant inhomogeneities within a single large sample, as well as temperature dependence when used at temperatures away from the design point. Zerodur has also been reported to show hysteresis that could potentially complicate modeling and analysis. The models described here used constant values for the material properties, with no time or temperature dependence.

Time Dependence

Time dependence in the modeled systems was addressed through transient thermal models, which were then used to drive the structural models. The thermal changes in the system occur slowly enough that the thermally induced structural deformations can be treated as quasi-static, and addressed simply by solving the structural model at various times of interest using snapshots from the transient thermal model as inputs.

The thermal problems in TOM and those currently being used for system design are slowly time varying, modeling maneuvers of several hours duration. The flight hardware under test, primarily the SID but also the CMP, are very well designed thermally. The primary thermal energy transport mechanism from the environment to the test articles is radiation and it far exceeds that transported by conduction. As a result, the fundamental time constants of the hardware (~10 hrs) are still short compared to the driving temperature change rates (~24 hrs).

Setting the initial temperatures for the thermal problem takes some care since it is not possible to easily start the model solution in thermal balance in a way that matches the physical hardware closely. In practice the solution is computed for several operational cycles and the last cycle is used for reporting. The cycle-to-cycle repeatability is determined and used in weighing assessment of reported results.

As a general observation, the thermal problem statement approximates the experiment. The active temperature controllers in the experiment on the cold walls and the heater cans are approximately modeled. In all cases used in reporting, the thermal analyst accepted these approximations and accounted for them in the interpretation of the results. The resulting temperature fields on the hardware are, by design, largely homogeneous and uniform in space and slowly varying in time.

Numerical Precision

One potential issue in the modeling of large systems, such as the SIM collector system, to such high precision is the possibility of the numerical methods themselves becoming a limitation on the quality of the modeling. These effects can appear as a result of roundoff or truncation errors that propagate into the more significant digits of the results during computations with many iterations, or they can be a function of the internal precision of the computer or software package.

The thermal problem is non-linear because of the T^4 term and must be solved in absolute temperatures, and is thus of concern, since we are working in mK around 293 K. The possibility of this causing difficulty was recognized early, and efforts were made to identify any possible issues. The manufacturer of TMG [ref to company] went through their code to verify how calculations were done, and provided the modelers with details of where single and double precision numbers were used, and how. The temperature problem is solved in double precision and the results are preserved until conversion to relative temperatures in single precision for the structural problem. Additionally, models were run under a variety of conditions and no signs of instability or unusual behavior of the tools was observed.

The structural problem is less of an issue because it is linear and is solved in relative temperatures. For a temperature time series, the driving structural temperatures for each step are relative to the first step. This reduces the required dynamic range of the model and relieves the pressure on floating point precision.

One minor issue related to numerical precision occurred when results were passed from one model to the next using a simple spreadsheet. The original data contained sufficient precision to produce stable results, but a quirk in the spreadsheet design caused them to be truncated, on import into the optical model, providing inaccurate results. This problem was easily corrected after being identified, but illustrates the care that needs to be taken in integrating the results across tools.

4. DEVELOPMENT OF THE SIM MODELS

The models used for analysis are developed largely from the hardware designs. The analysis models were

constructed to the design solid models and drawings that were used to fabricate the flight hardware. The brassboard hardware was fabricated to within specified limits, but the analysis models were not checked against the as-build hardware dimensions.

The analysis model mechanical material properties were tabulated values based upon accepted flight hardware rules using MIL-HDBK-5 (where available) and operating temperature range. Properties for athermal materials taken from best available accepted vendor or JPL sources. No time dependence was included in any material property, thermal or mechanical.

In some cases, where detailed modeling of a part was too complex or material properties were not well characterized, approximations were made in the models. The most significant of these are the SID CTE, which was not well characterized and is not uniform across the SID, ϵ^* of multi-layer insulation (MLI) thermal blankets, and SID heater can coating ϵ . The parameter ϵ^* is an effective radiative conductance of the MLI blankets used to avoid the complexity of modeling heat transfer through the many layers of the MLI.

Temperature predictions were transferred directly into an Ideas structural deformations model in order to calculate the resulting mirror wave-front error or OPD. This OPD prediction was then transferred over to an optics model in CODE-V to predict optical performance. This process of "integrated modeling" was refined so that minimal translation errors would result during the temperature mapping process. For the most critical temperatures, the SID mirror, DCC, and DCC post, the same finite element mesh was used in both the structural and thermal models so that there would be no interpolation error. A specialized MATLAB script was developed on the structures side to read in raw TMG output files to ensure that the results were read back into the structures model in double precision (the Ideas post processing environment reduces the number of significant digits used in the TMG solver).

Thermal Results Mapping

The thermal models use larger size elements than the finely meshed structural models, creating a challenge in mapping the temperatures obtained by the thermal model into the structural model. Using the I-DEAS software it was relatively simple to map the temperatures from the thermal model into the structural model. Within the I-DEAS Simulation, under the TMG Thermal Analysis application, there is a temperature mapping function that allows the user to map a temperature result set from one FEM to another. The temperature mapping tool uses spatial locations of nodes and elements to map temperatures from one model to another.

Figure 5 shows an example of a thermal model and the corresponding temperatures mapped into a structural FEM. It is also easy to see in the figure the element size used for each to the models.

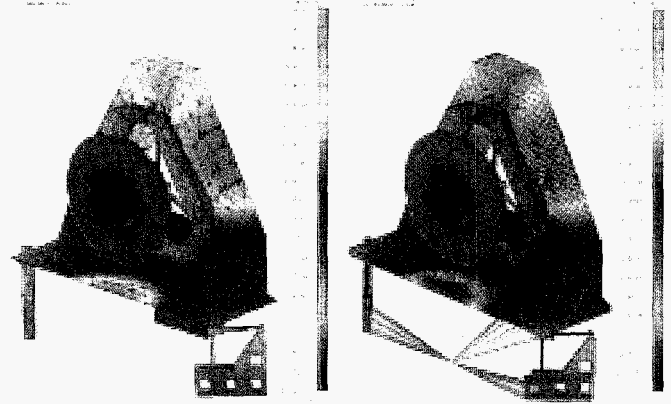


Figure 5 – Example FEM mapping of thermal (left) and structural (right) models.

5. COMPRESSOR MODEL AND VALIDATION

Due to the short schedule that was available for the TOM3 testing for SIM Milestone 8, the CMP wasn't expected to be available on time for testing and the testbed was designed so that the compressor would be outside the thermal shroud. This would have allowed the use of commercial optics on commercial mounts not designed for high thermal stability. During integration of the testbed, the CMP was delivered early enough to be integrated into the testbed and used for all of the SIM Milestone 8 testing.

Although it was not located in the thermal shroud the compressor was in a very stable thermal environment. In addition to the isolation of the vacuum chamber, it was also covered with MLI blankets and additional MLI blankets limited the view factor from the open side of the compressor to the chamber walls. The outside of the thermal shroud was also blanketed, preventing the compressor from seeing the cold LN2 shroud directly. The typical temperature variations of the compressor were ± 1 K/day. Thermal models of the flight system show that this is comparable in both rate of change and magnitude to the temperature variations expected during normal operation in space.

Thermal

Because the CMP was not in as tightly controlled a thermal environment as the SID, a mK model of the CMO was not developed. Instead, a simple 1 K thermal soak (uniform temperature change) was applied and the effects were calculated using the structural FEM and the Code V optical model. Only this one case was needed because all models use time and temperature independent material properties and larger temperature changes can be simply scaled from the 1 K case.

Compressor Bench Model

The FEM for the compressor bench was delivered by ATK [10], who also manufactured the the compressor bench. The model has 198,469 nodes and 254, 408 elements. The actual mass of the bench as delivered to JPL is 14.8 Kg, the FEM mass was calculated as 15.32 kg. Figure 6 shows the FEM of the ATK compressor bench.

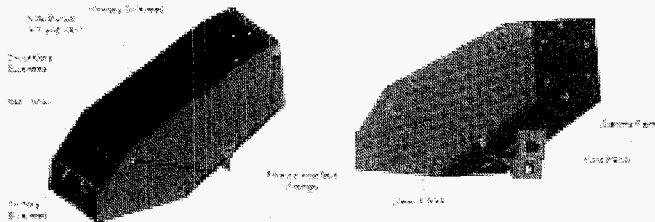


Figure 6 – Compressor Bench Structural Model.

The bench was constructed of composite material with Invar fittings. Material properties for Invar Type 2 were obtained from COI Database and Specification COPS-012. Material properties for the M55J/CE-3 laminate were calculated for 54% fiber volume using compressive modulus properties and from constituents using Composite Cylinder Assemblage Method and CLT. The properties were used for all faceskins and a majority of the ribs away from local bond lines and/or rib bonded intersections. Material properties which capture rib slotting and rib/skin bonds used effective properties. Effective properties assume a $_$ ” section around rib/adhesive interfaces, they also assume a nominal 0.015” bondline.

Material properties were assumed constant versus temperature because of the relatively small temperature range (-15°C to +60°C survival) required. In order to maintain the OPD below xxx, a CTE goal value between the primary and tertiary mirrors of 200 ppb/°C was specified. The effective CTE was then calculated as 89.6 ppb/°C from a thermal analysis with a 1°C temperature gradient applied to the bench.

Compressor Mirror Models

All mirrors inside the Compressor Bench, M1, M2, M3 and Fold Mirror (FM), were modeled at JPL. The picometer level models were created using solid, parabolic and linear, wedge and tetrahedron elements. The material properties were assumed to be constant with respect to temperature. The high fidelity FEMs for M1, the largest mirror in the compressor is shown in Figures 7.

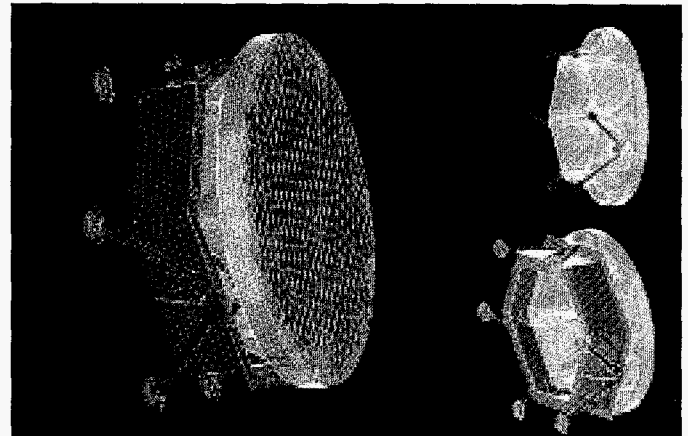


Figure 7 – Model of M1 (Compressor Primary Mirror) and mounts. Similar models were made of all four mirrors in the CMP.

M1 mirror has approximately 98,000 nodes and 49,000 elements. M2 has approximately 150,000 nodes and 79,000 elements. M3 has approximately 150,000 nodes and 46,000 elements. FM has approximately 20,000 nodes and 27,000 elements.

In order to provide results for the Compressor, the mirror FEMs had to be integrated with the Compressor Bench model from ATK. The first step was adding M1 and M2 to the Bench. A temperature steady state analysis was run. The model was very large, but the computer power was enough to run the case and provide results. Later on, the two additional mirrors M3 and FM were integrated into the model. Although the model was able to run, it was very slow, so it was separated into two pieces: one including the bench, M1, and M2, and the second including the bench M3 and the Fold Mirror. These models were run separately and the outputs integrated into a single deformation model.

Analysis of Print-through

A significant print-thru on the M1 mirror was observed at the manufacturer after the mirror was bonded to the JPL bipods and mount (Figure 8, top). The compressor with all mirrors mounted to it was delivered to the TOM3 team. The print-thru was also observed on the fully assembled compressor. An investigation into the M1 distortion problem was conducted at JPL.

Analyses of the distortion were carried out using the picometer level FEM of the M1 mirror, including gravity deformations, bonding shrinkage, thermal distortion analysis, etc. Several misalignment schemes were also analyzed. After the study was finished, it was determined that improper fixture support during surface figure measurements led to polished-in dimples. This problem was not detected at the manufacturer because of the fact that the mirror, being an offset parabola, was not rotated during the surface map measurements due to schedule constraints.

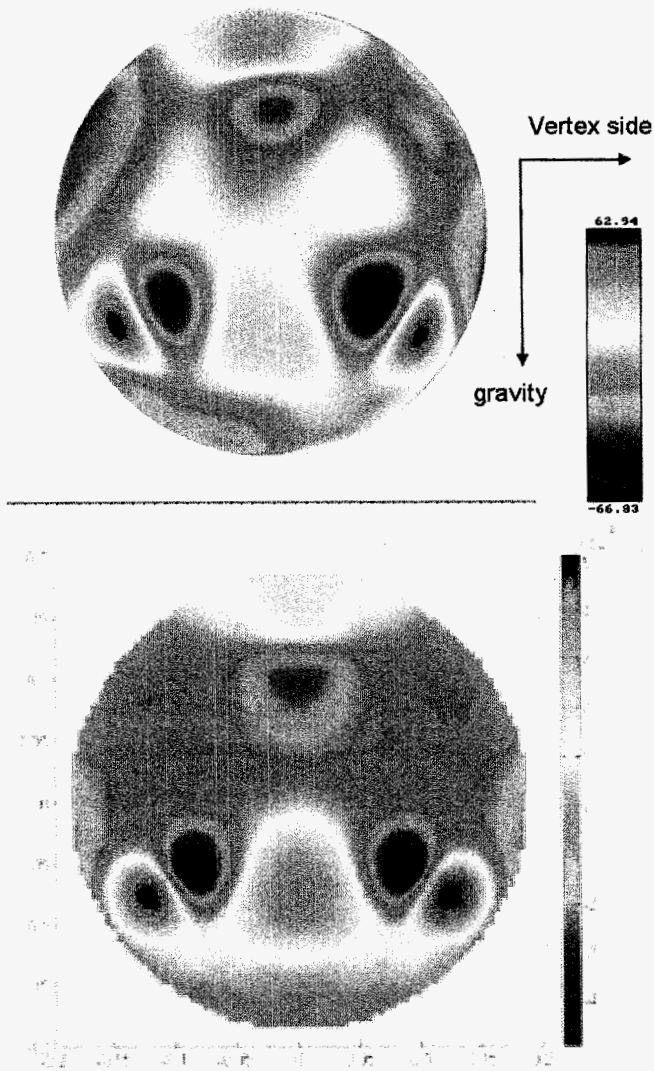


Figure 8 – M1 Mirror Print-Through showing 20 nm rms equivalent surface error, 129.8 nm peak-to-valley (P-V) (top). FEA combined case. M1 Mirror Analysis Results including 1 G gravity on bipods. Rms surface error is 14 nm, P-V is 103 nm. (bottom)

The analysis matched the shapes and amplitude (to the same order) of the measured error. The distortion mechanisms were also reviewed and concurred by the manufacturer. It is estimated that this problem accounted for about 2/3 of total distortion problem. Additionally, it was determined that inadequate mirror mount also contributed to the overall distortion. Wave front error (WFE) changes during shimming and mounting into the Compressor Bench were also observed, this problem was due to a soft offload ring and stiff supports (bipods, hexapods).

The combined finite element analysis (FEA) results for machined dimples, gravity sag and post-mounting hanging case are shown in the bottom of Figure 8. These results compared very well, both in magnitude and shape, with the mirror map shown in the top of Figure 8. The RMS values shown are within 30%, and the peak-to-

valley (P-V) values are within 20%. It is possible to obtain a better correlation of the results by identifying better values for some of the physical parameters, but in the interest of time the results were sufficiently convincing and were deemed appropriate.

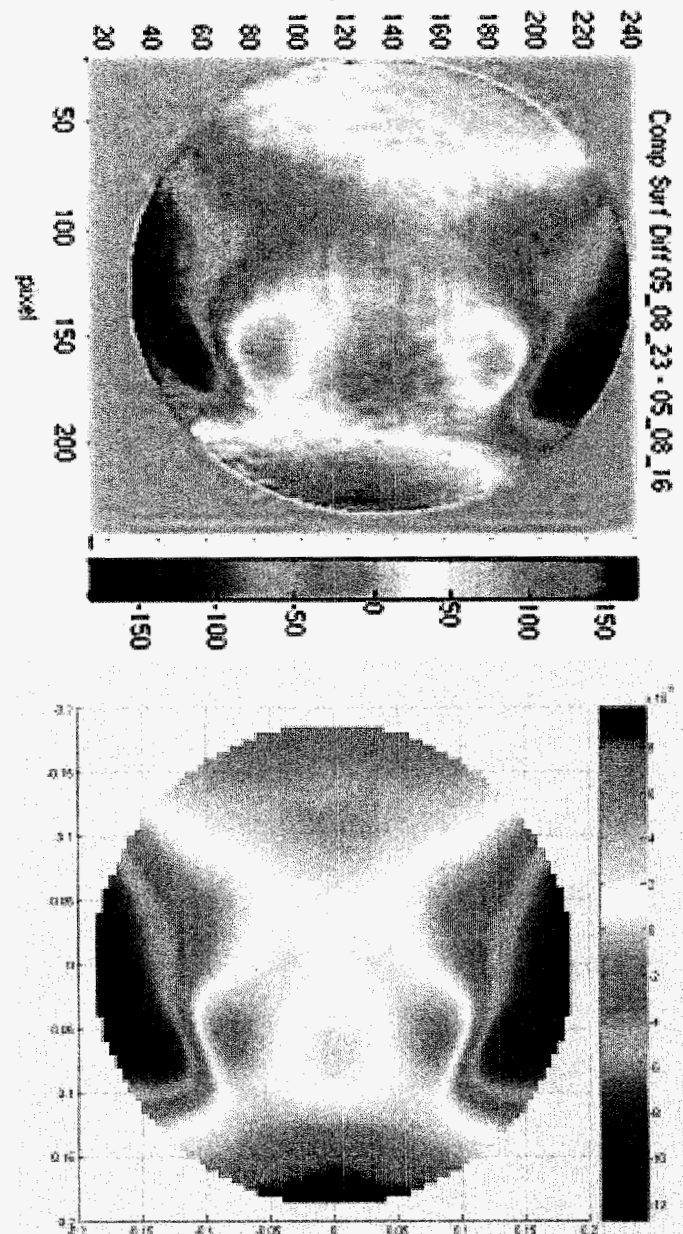


Figure 9 - M1 surface map measured during plunger test (top) and model results (bottom).

In order to verify the claim that the dimples were polished-in, a simple test was developed to try to remove the dimples from the glass surface. The test tried to mimic the force applied to the mirror by the measuring fixture at Tinsley, which produced a radial force equivalent to the mirror weight. For the test, two plungers were mounted on the side of the mirror, pressing the bipod mounts in the radial direction. Surface maps were obtained with and without the plungers and then

subtracted. The result is a map of the mirror with the plungers action only, without the effect of gravity, surface defects, etc. Figure 9(top) shows a map obtained from the TOM3 testbed and Figure 9 (bottom) shows the analysis results obtained by applying an equivalent force produced by the plungers on the M1 mirror. Visual analysis of the results shows good correlation between the two surface maps.

The RMS value for the measured map is 45.22nm and the P-V is 329.84nm. For the analytical results, the RMS value is 49.88nm and the P-V value is approximately 190nm. The P-V values are off by about 60% and this could be attributed to the uncertainty in the boundary conditions, as the force applied by the plungers could not be measured directly but was calculated from the manufacturers specification and the number of screw turns used to apply the force. At this time further investigation was not deemed required, since the main purpose of this test was to confirm that the testing fixture used during manufacture was indeed the culprit in creating the dimples.

Compressor Phase Map Analysis and Model Correlation

During the investigation of the M1 mirror print thru, a delta temperature soak case was also analyzed. During the TOM3 testing a temperature drop case was conducted and it was possible to perform a model correlation of the results.

Figure 10 (left) shows the surface map of the TOM3 M1 mirror after a 8.4 K temperature drop. Figure 10 (right) shows the analytical results due to an increase of 1 K in temperature. A visual analysis demonstrates an excellent correlation between the measured values and the analytical results. The RMS value for the tested article is 25.5 nm and a P-V of 240 nm. This translates to an RMS of 6.1 nm/K OPD error and a P-V of 14.25 nm/K surface error. The analytical results were calculated as RMS OPD error 7.2 nm/K OPD and a P-V surface error of 14 nm/K.

Compressor OPD Measurement and Model Correlation

In addition to measuring the temperature effects on the compressor from phase maps, the metrology system used for precision OPD measurements was used for similar correlations. These measurements were compared to a model of the full compressor, including detector locations.

The optical path for the compressor was modeled in Code V. Deformations of the optics were generated by applying a 1 K thermal soak in the structural FEM. Thermal soak effects were represented by matrices showing mirror surface deviations from their nominal shapes. The matrices showed deviations from the nominal position for a certain number of surface points (from ~1400 for the fold mirror to ~3400 for the primary mirror). The optical model calculated the OPD difference between the central detector and the other 9 COPHI detectors for the nominal and perturbed cases and the

OPD difference between these cases for each detector. Then, the average OPD change was calculated.

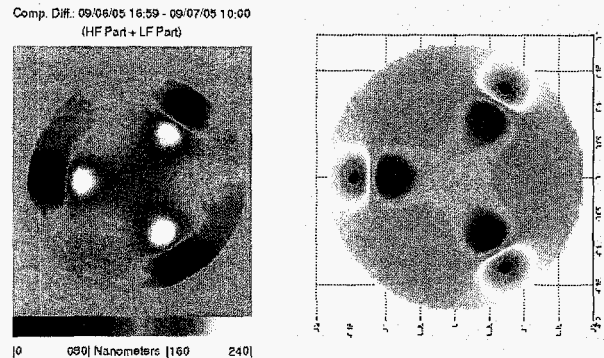


Figure 10 – Differences in phase map of the compressor compared to deformation map of the model with a 1 K soak. Distortion of Mirror after a Uniform Temperature Drop 8.4 K (measured, left). Uniform Temperature Increase of 1 K(Calculated, right)

As the rays aimed at detector centers do not necessarily intersect the mirror surfaces at the thermal model's grid points, the surface deformations are interpolated from the 3 nearest grid points by a separate Code V script called from within the main script. The program also allows introduction of X- and Y-beamwalk (in microns) which also affects the OPD change.

In comparing the model output to the experimental data, it was particularly important to ensure that the model accurately followed the experimental setup. Simply taking the average or RMS deviation of the surface would produce misleading results, as the mirror mounts provide a non-uniformity to the deformation of the surface, and the detectors only sample particular points on the surface.

When the proper position and alignment was used, the predicted OPD change was 9.97 nm/K, as compared to 8 nm/K measured value. Figure 11 shows the measured compressor OPD changes with temperature along with a line fit of 8 nm/K. Figure 12 shows the measured OPD changes of the CMP/SID system with the compressor diurnal effects removed by using the 8 nm/K and using the average temperature of the compressor from 5 thermometers.

These results are consistent with the phase map analysis thought slightly higher. Note that OPD results need to be divided by 4 to get the surface error, because the light from COPHI travels through the compressor twice for each measurement, once traveling to the chopping flat and once returning, and on each pass through the compressor traverses each mirror surface twice (once incoming, once outgoing).

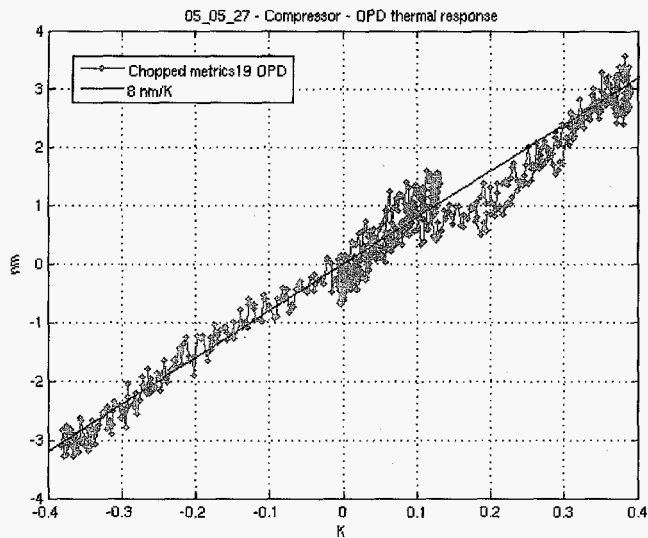


Figure 11 – Compressor Thermal Response as a function of temperature change.

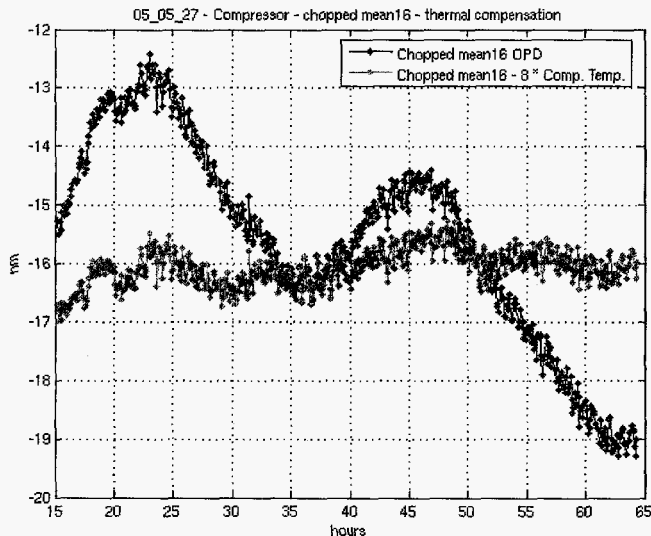


Figure 12 – Siderostat OPD change with time after subtracting diurnal variations of compressor using 8 nm/K and average temperature of 5° Thermometers distributed on the compressor.

6. SIDEROSTAT MODELING AND VALIDATION

Model

Ideas TMG was the chosen thermal package because of its level of integration with the structures and CAD communities on SIM. The mK thermal model shared direct associativity with CAD geometry in a TeamCenter CAD database. This ensured that the thermal, structures, and optical models would all be based off of one solid model representation and that all hardware representations in the models would occupy the same positions in space.

Figure 13 shows an exploded view of the mK thermal model of the SID.

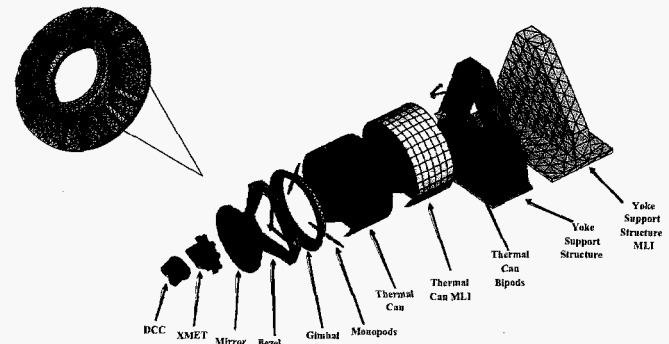


Figure 13 – mK Thermal model of the SID.

The SID mK thermal model was exceedingly detailed. A steady state thermal model run using a restart (re-using black body view factors) would take approximately 1/2 hour. A transient run simulating a TOM test would take approximately 8 hours. Often errors were discovered after thermal model runs had been made making the usability of the model difficult. For this reason, two other simplified models were developed of the test set up that would give answers more quickly. The first, a “facility-level” model was used for pre-test predictions of hardware time constants and required PID heater control constants.

Of more use, was the second 12-node SINDA/Fluint, TSS model used for quick calculations while tests were in progress. This model would run in approximately 10 seconds and would predict absolute temperature to within 5 C.

The thermal properties of the MLI and the SID heater can were modeled with a uniform property value, although the value was adjusted to early experiment results using the SID energy balance. This is effective because of the radiation dominance of the energy transport and the excellent thermal design of the SID.

The MLI is not explicitly modeled, but accounted for instead by using an effective emissivity e^* for the hardware surface protected. Differences between expected effectiveness of the MLI and the as-built performance are primarily due to MLI fabrication and installation effects. This is accepted flight project thermal practice because computing with faithful models of 30 layer MLI is not practical. Real world effects, such as stitching, surface condensation and staking, are significant and there is no established modeling technique to capture them. Standard practice, when tests are available, is to execute a few tests early to establish (aka tune) these parameters in well defined scenarios. Otherwise, bounded values based on prior flight project experience are used.

The emissivity of the SID heater can inner surface is the significant parameter in the radiative transport from the heater to the SID. The surface finish and color affect the value.

Thermal Model Correlation

The correlation process was started by first identifying the SID assembly's most sensitive thermal properties that would affect absolute temperature prediction with a thermal model. The simplified 12-node model was used for this purpose. These properties turned out to be Thermal Can MLI e^* (e -star, or effective MLI radiative conductance), Thermal Can heat flux, SID mirror emittance, DCC emittance, Aft Thermal Can internal emittance, bare ULE emittance. Using the mK thermal model, Torlon thermal conductivity was also found to be a sensitive variable. Sensitivity runs were completed with the simplified model for most of these parameters.

Once approximate values for each parameter were selected using the simplified model, the mK thermal model results were compared to one of the Technology Gate-8 steady state test cases. Table 1 shows a comparison between pre and post-correlation thermal parameters, and Table 2 shows some of the relevant parameters pre- and post-correlation.

Component	Material	ORIGINAL VALUES					POST CORRELATION				
		k (W/mK)	C _p (J/kgK)	ρ (kg/m ³)	ε	ε*	k (W/mK)	C _p (J/kgK)	ρ (kg/m ³)	ε	ε*
Aft Thermal Can	Al 6061-O	180	896	2700	0.1	0.09	180	896	2951	0.112	0.083
Forward Thermal Can	Al 6061-O	180	896	2700	0.06	0.03	180	898	2893	0.81	0.022
SID Mirror	ULE	1.31	766	2200	0.012/0.8	-	1.31	766	2146.28	0.027/0.78	-
DCC	Zerodur	1.65	812	2530	0.012	-	1.65	812	2528	0.027	-
DCC Post	ULE	1.31	766	2200	0.012/0.8	-	1.31	766	2153	0.03/0.81	-
Gimba Simulator	Al 6061-O	180	896	2700	0.1/0.86	-	180	896	2871	0.027/0.82	-
Passive TC Separator	Torlon	0.54	1000	1460	0.8	-	1.05	1000	2387	0.8	-
Base	Sup Invar 32-C	10.15	515	8140	0.8	-	10.15	515	8182	0.88	-

Table 1 – Pre- and Post-Correlation Thermal Parameters

	Temperature					dT/dt (mK/hr)				
	P-V Value (mK)		P-V Ratio		Uncorrelated Ratio (Model/Test)	P-V Value (mK/hr)		P-V Ratio		Uncorrelated Ratio (Model/Test)
	Test	Correlated Model	Correlated Model	Uncorrelated Model		Test	Correlated Model	Correlated Model	Uncorrelated Model	
SIDBCK1	17.6	20.2	1.15	1.06	0.9	10.2	0.6	1.0	1.03	
SIDBCK2	15.9	20.9	1.31	1.11	82	19.4	10.7	1.29	1.32	
SIDBCK3	18.7	24.9	1.33	1.17	7.7	12.3	11.7	1.60	1.52	
SIDSD1	18.1	22.1	1.22	1.13	6.9	11.0	10.4	1.56	1.61	
SIDSD2	18.3	24.1	1.31	1.20	7.4	11.9	11.3	1.61	1.53	
SIDSD3	18.5	25.6	1.38	1.30	7.5	12.5	11.9	1.67	1.59	
SIDBCKR1	17.4	21.2	1.22	1.12	7.0	10.8	10.1	1.51	1.44	
SIDBCKR2	18.0	22.5	1.25	1.17	7.0	11.2	10.7	1.60	1.53	
SIDBCKR3	18.8	19.0	1.01	1.04	6.9	9.9	9.2	1.39	1.33	
DCCW1	10.6	10.0	0.94	0.93	4.7	6.4	4.4	1.30	0.94	

Table 2 – Pre- and post-correlation temperature differences and rates of change on the SID.

It was immediately apparent that the pre-correlation choice of e^* was significantly different from what was needed to correlate the model. Given the Thermal Can's round geometry however, this value is still physically acceptable. Table 3 shows a comparison between thermal model absolute temperature predictions and TOM test results.

PRT Label	Sensor Location	Element Number	Test (K)	Model (K)	Delta (K)
SIDBCK1	SID Mirror, On Back (-X)	39629	293.0	293.2	0.2
SIDBCK2	SID Mirror, On Back (+X)	37237	292.5	292.8	0.3
SIDBCK3	SID Mirror, On Back (-Z)	38433	292.4	292.5	0.1
SIDSIDE1	SID Mirror, On Back Near Edge (-X)	39628	293.7	293.4	-0.3
SIDSIDE2	SID Mirror, On Back Near Edge (+X)	37236	293.3	293.1	-0.2
SIDSIDE3	SID Mirror, On Back Near Edge (-Z)	38432	293.2	292.9	-0.3
SIDBCKR1	SID Mirror, On Back Raised Portion (-X)	38796	292.8	293.3	0.5
SIDBCKR2	SID Mirror, On Back Raised Portion (+X)	37834	292.7	293.1	0.4
SIDBCKR3	SID Mirror, On Back Raised Portion (+Z)	40192	293.1	293.7	0.6

Table 3 – Absolute temperature predictions and experimental results.

Transient temperature correlation focused on two main thermal parameters, Thermal Can heater control constants and material capacitance. TMG does not have a PID heater control routine included. It was decided that since the hardware had such a large time constant, that just

simulating proportional heater control would match the test data good enough. The proportional constant was changed until the Aft and Forward Thermal Can boundary temperatures matched the test data closely. No further correlation was done until by request of the structures analyst, the ULE and Zerodur capacitance values were reduced by 5% to increase the predicted OPD. Figure 14 shows transient model prediction both pre and post correlation. Absolute temperature predictions have been offset from raw model output by approximately 1C.

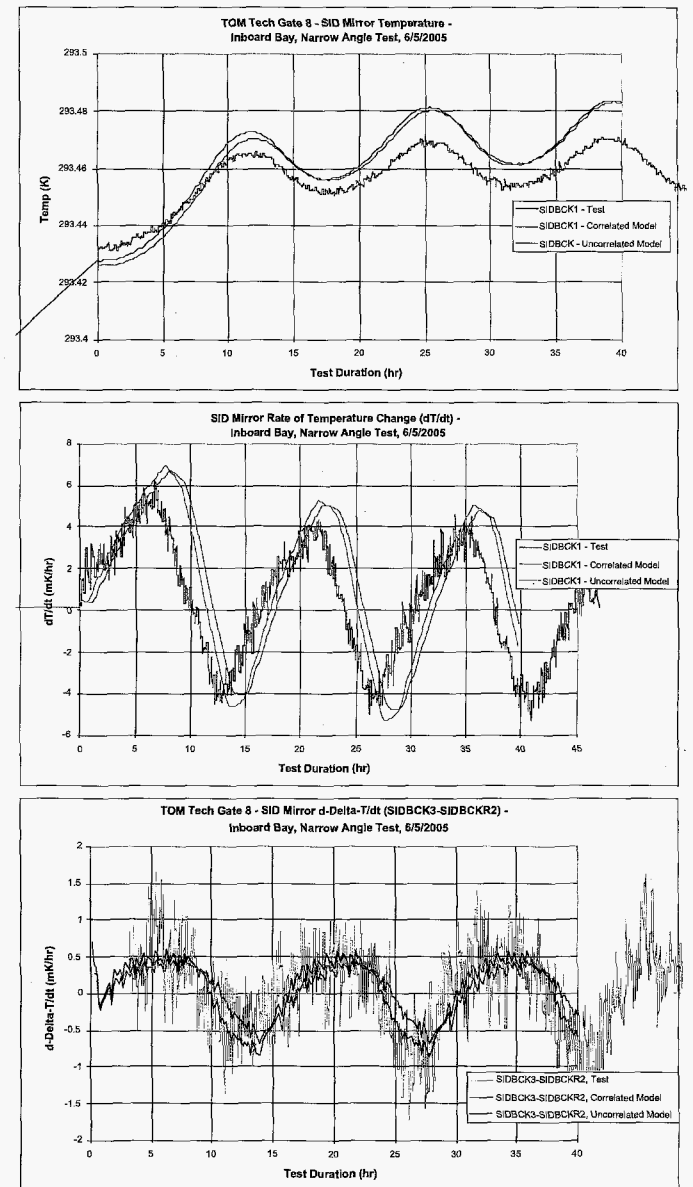


Figure 14 – Siderostat Predicted Temperatures – inboard narrow angle (top). Predicted Temperature Rate of Change for the inboard narrow angle case.(middle). Predicted Temperature Gradient Rate of Change – Inboard Narrow Angle (bottom)

SID Structural Modeling

As described earlier, structural models were developed in I-deas from the hardware designs and were designed to

map integrate with the thermal models. The Compressor Bench FEMS were provided by ATK, who also designed and manufactured the Compressor Bench. The FEMs of the compressor optics and their support structures were developed at JPL and integrated with the high fidelity FEM of the bench that ATK provided.

SID Model

Figure 15 shows the FEM developed for the SID. This model has 47,000 elements and 168,000 nodes. The actuator mechanisms were modeled as elastic beams. The model also contained the bipod supports which in turn were connected with rigid elements to a ground point.

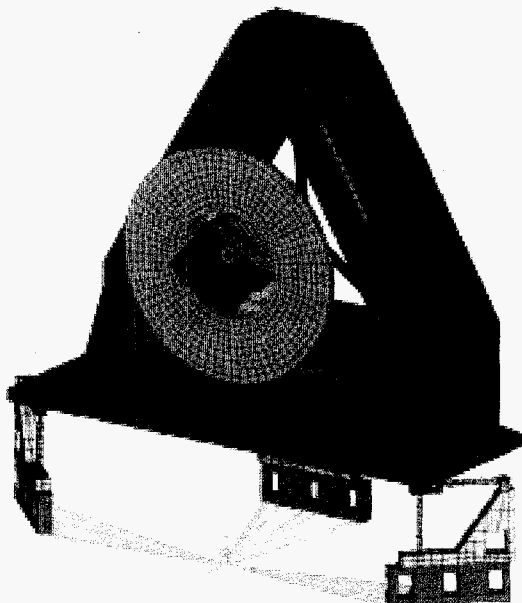


Figure 15 – SID Structural Model.

The SID mirror material is ULE, the DCC is made out of Zerodur and the rest of the structure is Invar. During the manufacturing process it was determined that the ULE's coefficient of thermal expansion (CTE) was not homogeneous throughout the material and thus it was required to develop an algorithm to allow the model to have heterogeneous material properties. A computer script was developed and successfully applied to the FEM to provide for varied CTE properties in the SID mirror.

Materials

Well established experience with certain materials e.g. aluminum, justifies uniformity. Most materials in the hardware are less well known ie Super Invar (SID bezel and bipods), Zerodur (DCC), and ULE (the SID mirror material). These are boutique materials engineered for zero CTE and suspected to exhibit non-uniform spatial properties, but no significant time dependent behavior is suspected in the operating temperature range. The SID mirror ULE properties are known to have spatial variation and available measured data still has significant uncertainty. The SID bezel material, Super Invar, has questions about its CTE due to heat treatment. The DCC

is Zerodur and has a remaining uncertainty about the sign (+ or -) on the CTE and a thermal cycle test has been proposed to determine the effect of DCC Zerodur CTE hysteresis on OPD performance.

Predictions and Validation

Because the SID is a simple optical flat with a retroreflector in the center, the OPD changes predicted are directly proportional to the thermally induced deformations and the experimental data can be compared to the model output without using an optical modeling tool. There is a factor of 2 to account for between surface deformations and OPD, because the optical path traverses each deformation on the SID twice—once incoming and once outgoing.

Figures 16 and 17 show the predicted OPD variations with time for two the test runs, along with empirical data.

OPD predictions were made in three different ways: fully modeled, in which thermal model predictions were made and put into the structural model to generate OPD outputs; partially modeled, in which an empirical value of OPD as a function of SID temperature was measured and simply multiplied by the temperatures from the thermal model; and empirically modeled, in which the previously measured $dOPD/dT$ number was simply multiplied by the measured temperature changes.

These results suggest that detailed knowledge of CTE values is very important in developing accurate models for the SID. The partially modeled and fully empirical predictions use the temperature difference between the DCC and the SID mirror, which crosses the boundary between two different materials, Zerodur and ULE. Both materials have very low CTE whose sign can be + or -, and which can vary from sample to sample of the material. Additionally, the CTE of ULE is inhomogeneous, and due to constraints in manufacturing neither the particular Zerodur nor ULE sample used in the SID are well characterized. Despite this, the models show that OPD changes can be predicted *a priori* to within about a factor of 2, which is acceptable for these components of SIM. Careful characterization during manufacture or testing at intermediate stages of fabrication might improve this predictive capability at reasonable expense. Further, the close correlation of the OPD to the temperature difference from the DCC to the SID might offer the capability of further reducing thermally induced errors in the completed system, even if they can't be perfectly predicted prior to assembly.

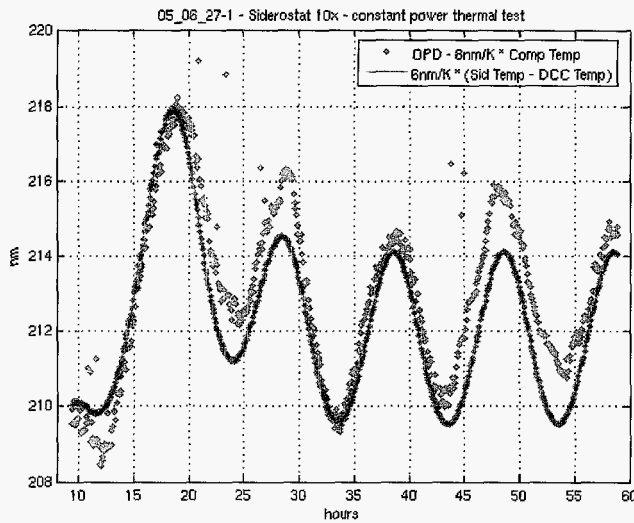


Figure 16 – SID Optical Path Difference data and empirical model fit.

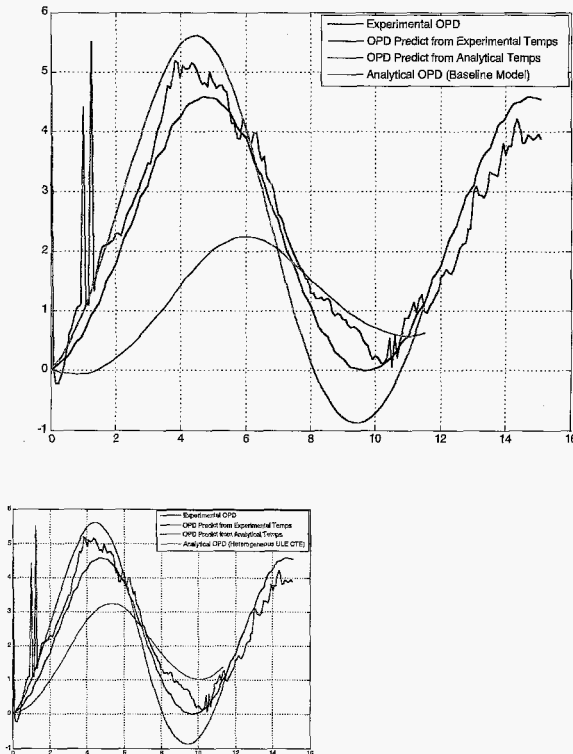


Figure 17 – SID OPD data compared to several models. See text for description of models.

7. CONCLUSIONS

Model Development

These results show that the integrated modeling process using is working and allows thermo/opto/mechanical modeling at levels needed for SIM. The process takes

advantage of commercially available FEA tools without need for additional tool development-- only process development for practical work and model flow. This is particularly valuable in minimizing development cost and time that would be incurred with custom tools or modified commercial tools.

In addition to benefiting from validation work that has gone into the commercial tools, the model and tools are being validated against experimental data at the precision required for SIM flight system development, confirming their applicability and usefulness for SIM.

Model Validation for SIM

The TOM3 testbed was successful in demonstrating the performance required for SIM Milestone 8 as well as providing models validation that allows reasonable margins to be assigned during flight system development.

The thermal models using the best available inputs predicted the relevant parameters (peak-to-valley temperature change and rate of change) to within 60% prior to any attempts to adjust model parameters to fit the experimental data. For most components of interest, except for the DCC, the model overpredicted the temperature swings and rate of change. After relatively small adjustments that are physically reasonable, the model consistently matches the experimental results or overpredicts by 20 to 60%. The overprediction is preferable to underprediction because it provides margin against design or modeling errors. It is also preferred that the model overpredict by a relatively consistent amount in order to simplify the assignment of margins and model uncertainty factors.

The structural models are fairly sensitive to accurate knowledge of material parameters, particularly CTE, but also provided performance predictions that are valuable for flight development. Prior to model correlation, the structural model of the SID underpredicted by a factor of about 3. After modifying the CTE of the ULE glass in the model to be more consistent with the properties of the real glass, including inhomogeneity, the model underpredicted by a factor of about 1.6. Although overprediction would be preferred, this very reasonable and also gives us a modeling uncertainty factor that is useful for developing design margins for the flight system that aren't prohibitively conservative.

These data, combined with an empirical model of the SID system also suggest that a combination of more detailed knowledge of material properties, possibly combined with tests at the component and subsystem level, can improve the fidelity of the models for use in design modifications or for integration into higher level models.

REFERENCES

- [1] <http://SIM.jpl.nasa.gov>, also Unwin, S. & Turyshev, S. 2004, JPL publication 2004-19
- [2] Science Overview and Status of the SIM Project Shao, M. 2004, SPIE 5491-36
- [3] Space Interferometry Mission (SIM)-technology completion and transition to flight, Laskin, R. 2004, SPIE 5491-37
- [4] R. Goullioud, C. A. Lindensmith, I. Hahn, Results from the TOM3 testbed: optics thermal deformation at the picometer level.
- [5] Zhao, F. Development of High Precision Heterodyne Metrology Gauges, in Advanced Sensor Systems and Applications II, edited by Yun-Jiang Rao, Osuk Y. Kwon, Gang-Ding Peng, Proceedings of SPIE Vol. 5634, p247-259 (SPIE, Bellingham, WA, 2005)
- [6] Zhao, F., Logan, J. E., Shaklan, S., Shao, M. A Common-Path, Multi-channel, Heterodyne Laser Interferometer for Nanometer Surface Metrology, in proceedings of OSJ/SPIE Conference on Optical Engineering for Sensing and Nanotechnology (ICOSN '99) • SPIE Vol. 3740, p 642-645 (Yokohama, Japan • June 1999)
- [7] UGS Corporation, Plano, TX 75024. Also <http://www.ugs.com>.
- [8] Maya Heat Transfer Technologies, Ltd, Montréal, PQ, Canada, H3Z 1T3.
- [9] Optical Research Associates, Pasadena, CA 91107.
- [10] ATK Space Systems, San Diego, CA 92121

missions and instruments, including the Planck mission, the JWST mid-IR instrument, and a next-generation microwave limb sounder. He also led the development and demonstration of 6 K sorption cryocoolers at JPL. He has a PhD in physics from the University of Minnesota, where he performed research on the nucleation of quantized vortices in superfluid helium, and a BS in physics from the University of Michigan. In between his BS and PhD, he spent two years at American Superconductor in Cambridge, MA, working on the early development of high-temperature superconducting wire.

BIOGRAPHY



Chris Lindensmith is a system engineer for the collector subsystem on SIM Planetquest. He has served as project technologist on the Terrestrial Planet Finder mission and as the lead system engineer on TPF during the development of earlier mission concepts leading to the current two. He started at JPL in 1996, working on the development of cryogenic technologies, including magnetostrictive actuators. Since then he has supported development of

End of File

